Evaluation of an Adaptive Control Algorithm for use in Uniform Droplet Spray in Droplet Based Manufacturing

by

Samuel Thurston Towell

Submitted to the Department of Mechanical
Engineering in Partial Fulfillment of the
Requirements for the
Degree of

Bachelors of Science

at the

Massachusetts Institute of Technology

May 2000
[June 2000]

Signature of Author..
Department of Mechanical Engineering
May 5th, 2000

Certified by..
Jung-Hoon Chun
Associate Professor of Mechanical Engineering
Thesis Supervisor

Accepted by..
Ernest G. Cravalho
Professor of Mechanical Engineering
Chairman, Undergraduate Thesis Committee

Evaluation of an Adaptive Control Algorithm for use in Uniform Droplet Spray in Droplet Based Manufacturing

by

Samuel Thurston Towell

Submitted to the Department of Mechanical Engineering on May 5th, 2000
in Partial Fulfillment of the Requirements for the Degree of
Bachelors of Science

ABSTRACT

This thesis presents the results of a simulation study comparing the current integral control system with an adaptive control system for potential use in a Uniform Droplet Spray Process. First, an adaptive control algorithm was derived. Then, this algorithm and the existing integral control algorithm were coded for use in MATLAB simulations. The simulations were performed against each other over various sampling periods and noise classes to compare the performance of both droplet diameter mean and standard deviation. Results showed that for the target diameter of 760 μm, the adaptive controller could produce droplets with the mean diameter of 759.9 μm and a standard deviation of 0.0066 μm, while the integral controller produced droplets having the mean diameter and standard deviation of 759.7 μm and 0.0084 μm, respectively. Over the sampling periods experimented with, the adaptive controller could produce droplets with the mean diameter of 759.9 μm and a standard deviation of 0.0061 μm, while the integral controller produced droplets having the mean diameter and standard deviation of 759.9 μm and 0.0074 μm, respectively.

Thesis Supervisor:
Dr. Jung-Hoon Chun
Associate Professor of Mechanical Engineering

Acknowledgements

I would like to thank all the persons who made possible the completion of this work. My most sincere gratitude to:

Professor Jung-Hoon Chun, for taking me on as an undergraduate thesis student and for his encouragement and support throughout this process. Jeanie Cherng for her help in the laboratory and for her expertise in the details of MATLAB. Dr. Jae-Hyuk Oh for the use of his initial ideas for the project and for his continuing support throughout the term. And finally to my father and mother, who have given me unconditional support and encouragement from home throughout my life and more especially during my four years at the Massachusetts Institute of Technology.

To you all,

Thank you very much

Table of Contents

List of Figures and Tables

Page

List of Tables

List of Figures

1. Introduction

The scope of the research contained in this thesis centers around computer simulations of a control system designed to improve the pre-solidification production of solder spheres in a Uniform Droplet Spray (UDS) apparatus. The current integral control system is modeled in MATLAB resulting in an accurate representation of droplet formation under current UDS process conditions. Based on the assumptions of that model a second simulation was constructed around an adaptive control algorithm. Such an algorithm is believed to filter systematic noise in a more reliable fashion than an integral controller. The purpose of this investigation is to determine the potential merit of such a control system based on both the current sensor configuration and the possibility of a sensor system with a shorter sampling period.

These simulations are constructed to test the controllability under two primary conditions: white noise and Gaussian noise. There is reason to believe that the latter element provides justification for an adaptive system, that is to say, a system that can use past information to predict upcoming systematic variations. The simulations are designed to quantify the advantage of such a system in the presence of variations that have previously been modeled as constant but may in fact vary to some unknown degree.

In this work, the algebraic equations governing the size of the metal droplets were derived. Then, these expressions were broken down for implementation into an adaptive control algorithm. Next, both the existing integral control system and the adaptive control system were modeled in MATLAB. The simulations were run under similar conditions and tested for both the mean and standard deviation of droplet diameters formed in the presence of white and Gaussian noise.

2. UDS Process

As the drive for faster processing speed continues, electronic components are continually redesigned to be smaller, faster and denser. It is this last element that is of special concern to this particular project. A greater number of Input/Output connections per unit area correlates to a smaller overall chip while maintaining the same performance. Ball Grid Array (BGA) technology presents a possible avenue of development beyond the chip configurations that currently exist. Most prominent among conventional technologies are the quad flat pack array (QFA) and the pin grid array (PGA) chips. The latter was developed in the 1960s and has great interconnection flexibility. The geometry of the pins allows for a great many contact points in a given area but at the cost of a reduced potential for pitch reduction. QFAs use flatter, wider connective devices, solving some of the problems found in the PGA arrangement. However, the connector number is far lower and there are serious size restrictions as a result of the peripheral geometry of the prongs.

BGA technology brings with it the potential for smaller devices at lower cost. In some cases the size reduction can be as great as fivefold. The metal spheres are used as the connective devices and allow for higher densities compared to other current methods. Of additional interest is the lower defect rate in production, especially when compared with a device such as the PGA chip. Because of its superior qualities and higher reliability, it is believed that BGA technology could become the standard in the field of wafer and chip manufacture within the foreseeable future [Rocha, 1997].

The spheres used in BGA technology can be created through a variety of methods. Currently, the most promising appears to be the Uniform Droplet Spray process. The apparatus for such a process is composed of a Pyrex chamber, a crucible chamber, a control system, and a heater. The crucible chamber houses all droplet-generating functions (see Figure 1). It is here that the metal is melted. The melt is forced through a sapphire orifice in the bottom of the chamber by pressurized inert gas. This results in a laminar molten metal jet. This jet is disturbed by a shaft and disk connected to a piezoelectric stack. The frequency of oscillation of the stack determines the diameter of the droplets generated by the break up of the laminar jet. After breaking up, the individual droplets fall through a charging plate that places a positive charge on each one. This causes them to repel each other and prevents them from merging as they fall. The spheres begin to solidify as they fall, and the solidification process is completed as the spheres are collected in an oil bath, or, if in an inert environment such as Nitrogen, at the end of flight [Chun et al., 2000].

A computer running a visual basic script governs the control system. The data is taken by a CCD camera/strobe light combination located near the orifice of the crucible chamber. The output of the computer is sent to a function generator that drives the piezoelectric stack with the assistance of an amplifier and a transformer. An oscilloscope is connected in parallel for user convenience. The entire schematic can be viewed in Figure 2.

The current control system design uses an integral controller in conjunction with standard image acquisition software. A CCD camera takes images of produced droplets within five centimeters of the orifice. The droplets are backlit by the strobe light at a certain frequency corresponding to the speed of the data and image acquisition software package of the controlling computer. The strobe, flashing at one-tenth the breakup frequency, freezes the image of the droplets in space for the data acquisition package.

The captured image is then analyzed to determine the produced metal droplet diameter. The strobe light provides a strong contrast between the dark droplets and a resulting white background. The image acquisition process uses this contrast to perform an edge detection function on the image, thus obtaining an approximation of the diameter of the droplet. Using this information, the control system is able to adjust the breakup frequency to bring the actual diameter closer to the target diameter.

The present UDS process uses integral control to reduce droplet size variability. At its most basic level, integral control is the correction of an observed discrepancy with a target value by the addition or subtraction of that error multiplied by a predetermined gain [Kuo, 1975]. Within the UDS, this corresponds to the measurement of a produced metal droplet diameter, a comparison of that value with the target diameter, and, based on that discrepancy, a modification the driver frequency accordingly.

The governing equations of the droplet diameters are tied to both the intrinsic properties of the material and the processing conditions in the crucible chamber under which the spheres are produced. This diameter, *d*, can be expressed as [Rocha, 1997]:

$$d = \left(\frac{9 c_n^2 d_O^2 \rho_l}{2 \rho_s^2} \right)^{\frac{1}{6}} \left(\frac{p + \rho_l g h}{f^2} \right)^{\frac{1}{6}}, \tag{1}$$

where c_n is the discharge constant, an empirically determined value based primarily on the orifice diameter, d_O, and the pressure, p. The densities of the material in liquid and solid form are given by ρ_l and ρ_s, respectively. The remaining factors are gravity, g, the breakup frequency, *f*, and the height of the material, in liquid form, in the crucible, *h*. The first term on the right-hand side of Equation 1 remains constant throughout the process. It contains the parameters affecting the state of the metal and the dimensions of its container. The second term includes the two applicable elements from Bernoulli's equation for flow present in this configuration, pressure and molten metal head. It is also in this term that one can observe the relationship between the breakup frequency and the diameter of the resulting droplet. To simplify further calculations, the first term on the right hand side of the equation can be reduced to a constant called c_o:

$$c_o = \left(\frac{9 c_n^2 d_O^2 \rho_l}{2 \rho_s^2} \right)^{\frac{1}{6}}. \tag{2}$$

This constant can be withdrawn in all further calculations. An additional convenience will be the introduction of ξ, where:

$$\xi = f^{-\frac{1}{3}}. \tag{3}$$

The simplified expression for droplet diameter is as follows:

$$d = c_o \left(p + \rho_l g h \right)^{\frac{1}{6}} \xi. \tag{4}$$

3. Adaptive Controller Design

In a general sense, an integral closed-loop control can be modeled as:

$$f(t) = K\int_{0}^{t} e(t)dt \tag{5}$$

where the frequency changes at a rate proportional to the integral of the error signal. Here K is the gain by which the error signal is multiplied. This gain must be empirically deduced and needs to be recalibrated for each ball size. The integral control system is reasonably robust, generating spheres within 3% of the target diameter. Given an initial frequency, the controller can bring the ball diameter back within control in under six seconds. In MATLAB, this control script takes on the following form,

```
error=(Ddr*1e6)-(TD);
freq(i,1)=frequency;
frequency1=frequency;
frequency=frequency1+(g)*error;
```

Here (g) is the constant gain (equivalent to K in Equation 5). The entire code can be seen in Appendix A.

The use of adaptive control, while not strictly dynamic, takes a more holistic approach to the UDS control system. This algorithm encompasses not only the target diameter and frequencies as inputs, but also those empirically derived elements that had previously been held constant for purposes of simplicity [Kuo, 1975]. By allowing those values, taken together as a holistic constant, to fluctuate over time, a more accurate frequency could be obtained to produce desired ball diameters.

The molten metal height cannot initially be taken as constant, and is related to the velocity of the jet stream exiting the UDS apparatus, υ_J, in the following way [Yim, 1996]:

$$\frac{dh}{dt} = -\frac{d_O^2 \upsilon_J}{d_C^2}, \tag{6}$$

where d_C is the inner diameter of the crucible. It can be shown that this jet stream velocity, υ_J, can be expressed in the following manner:

$$\upsilon_J(t) = c_n \sqrt{\frac{2(p + \rho_l g h(t))}{\rho_l}}. \tag{7}$$

as it is only a function of the variables from Bernoulli's Equation for laminar flow acting on the material itself in the liquid state.

By integrating Equations 5 and 6, the following expression can be obtained:

$$\sqrt{p + \rho_l g h(t)} = \alpha + \beta t. \tag{8}$$

Equation 8 is the basis from which the adaptive controller's usefulness is derived. While gravity and the liquid density of the material remain constants, fluctuations in both the height of the melt and the pressure acting on the system can now be taken into account from the controller's point of view. Individual monitoring systems need not be installed for these two variables because they are taken together in the expression $\alpha+\beta t$. Further examination of this expression reveals the following:

$$\alpha = c_0^3 \sqrt{p + \rho_l g h_0} \tag{9}$$

$$\beta = c_0^3 \frac{\sqrt{\rho_l} c_n g d_J^2}{\sqrt{2} d_C^2}. \qquad (10)$$

Here α is the expression encompassing the initial state of the melt in the crucible, and β is the dynamic effect of the change in the melt height. Taking all the aforementioned changes into account, the original expression for the sphere diameter can be expressed as:

$$d = (\alpha + \beta t)^{\frac{1}{3}} \xi. \qquad (11)$$

Using Equation 11, an adaptive controller should help bring the actual diameter closer to the target diameter by addressing the effects of both noise and disturbances in melt height and chamber pressure. The controlled variable, ξ, is now separated from the rest of Equation 11 and can respond to variations arising from any part of the equation within the parentheses. Through this "black box" approach none of the elements previously held constant are varied individually. Rather, the terms α and β, comprised of these elements are adjusted over time in an adaptive manner; that is to say, the two variables may not accurately represent the true values of the variables that constitute them, but the changes they undergo assist in the ultimate goal of bringing the sphere diameter closer to the target value.

To get a more accurate error evaluation, a mean squared error approach was taken. This method results in higher error definition. By setting Equation 11 to zero, and squaring the absolute value, the following equation results:

$$J = \sum_{i=0}^{n} \left| d(i)^3 - (\alpha - \beta i T)\xi(i)^3 \right|^2 \qquad (12)$$

For the purposes of error control, J in Equation 12 must be minimized. In order to give the adaptive control a time history with which to work, α and β must be modified over time. Since the only control input into the system is the frequency, which manifests itself in ξ, both α and β need to use continuous information.

$$\begin{bmatrix} \alpha(n) \\ \beta(n) \end{bmatrix} = \begin{bmatrix} \sum_{i=0}^{n} \xi^6(i) & -T\sum_{i=0}^{n} \xi^6(i) \\ -T\sum_{i=0}^{n} \xi^6(i) T^2 & \sum_{i=0}^{n} \xi^6(i)^2 \end{bmatrix}^{-1} \begin{bmatrix} \sum_{i=0}^{n} \left(\xi(i)d(i)\right)^3 \\ -T\sum_{i=0}^{n} \left(\xi(i)d(i)\right)^3 i \end{bmatrix} \tag{13}$$

Equation 13 shows a matrix implementation of Equation 12. This matrix grows over time with the addition of each previous ξ, allowing for systematic discrepancies to be eliminated as well. This adaptive control takes on the form of Equation 14 below:

$$\xi(n+1) = (\alpha(n) - \beta(n)(n+1)T)^{-\frac{1}{3}}. \tag{14}$$

The implementation of such an expression can be seen in the MATLAB code below.

```
 u(i)=frequency^(-1/3);
An=An+u(i)^6*[1 -T*(i); -T*(i) (T*(i))^2];
Bn=Bn+u(i)^3*Ddr^3*[1; -T*(i)];
X=(inv(An)*Bn);
u(i+1)=(X(1,1)-X(2,1)*(i+1)*T)^(-1/3)*Ddr;
```

The entire procedure can be seen in Appendix B. Note the similarity in the construction of the droplet generating code in both cases. This is to ensure that the controllers are both responding to identical fluctuations.

In order to create a realistic timeframe over which to use historical data, a variable window size was integrated. This prevents the controller from attempting to handle the entire frequency data matrix at each update. This feature can be observed in Appendix C. The larger the window size, the more data the controller has available with which to adapt to the breakup frequency. However, this window size may be limited by physical constraints. The larger the windows require the code to process greater amounts of data to determine the new frequency.

For the purposes of comparison, both the adaptive and the integral controller were placed under similar conditions in a MATLAB simulation. Of primary concern was the accurate modeling of the process conditions in which the system was to control. The inputs to the program itself were the target diameter, the orifice diameter, the pressure in the crucible chamber, the initial vibration frequency of the piezoelectric stack, the weight of the metal, in solid form, that would be used for the melt, the duration of the simulation, the sampling period, the error level inherent in the system, the gain for the integral controller, and the window size for the adaptive controller [Rocha, 1997].

Table 1: Initial Conditions of Simulations

Variable	Integral	Adaptive
Target Diameter (μm)	760	760
Orifice Diameter (μm)	406	406
Pressure (psi)	5	5
Initial Frequency (Hz)	1500	1500
Metal Weight (kg)	0.5	0.5
Simulation Duration (s)	120	120
Sampling Period (s)	0.8	0.8
System Noise	0.025	0.025
Gain	3	-
Window Size	-	25, 50, 75, 100

As Table 1 shows, the initial conditions for the two simulations are almost identical. The only differences lie in the final two parameters that are specific to the controllers themselves.

4. Controller Simulations Results and Discussion

Figure 3 shows the performance of both controllers in the MATLAB simulation in the absence of noise. The adaptive controller performed better in the simulation with a sampling time of 0.8 seconds. The droplet diameter settled to exactly 760 μm in the adaptive case while the integral controller reaches a peak of 759.7 μm. It also took the integral controller 5 seconds to reach a steady-state value. The adaptive controller reached its steady-state value in 0.5 seconds. Neither run showed overshoot.

Next, the controllers were compared in the presence of white noise (Figure 4). White noise is modeled by generating random numbers in a uniform distribution and fitting them within the error range determined empirically from the UDS process itself. The noise profile was saved to allow both controller simulations to use the same one, therefore more tightly controlling the experiment. Consistently through the simulations the adaptive controller deviated less from the target diameter in response to the error noise than did the integral controller. The results are presented in Table 2.

Table 2: Controller response simulations to white noise

Integral		Adaptive		
Mean Diameter (μm)	Standard Deviation (μm)	Mean Diameter (μm)	Standard Deviation (μm)	Window Size
759.7	0.0075	759.8	0.007	25
759.7	0.0075	759.8	0.0067	50
759.7	0.0075	760	0.0067	75
759.7	0.0075	760	0.0065	100

The next comparison involved Gaussian noise. This distribution is believed to more accurately model the noise that is caused from the system as opposed to the uniform distribution of the white noise. The resulting responses are presented in Figure 5. Once again the adaptive controller's tighter variance is evident in almost every data point. Both the sphere diameter standard deviation and mean are more variable than in the white noise scenario. A complete evaluation of the results is available in Table 3.

Table 3: Controller response simulations to Gaussian noise

Integral		Adaptive		
Mean Diameter (μm)	Standard Deviation (μm)	Mean Diameter (μm)	Standard Deviation (μm)	Window Size
759.7	0.0084	759.6	0.008	25
759.7	0.0084	760.1	0.007	50
759.7	0.0084	760.3	0.007	75
759.7	0.0084	759.9	0.0066	100

The final point of comparison between the controller simulations involved the reduction of the sampling period. Sampling periods of 0.6, 0.4, 0.2, 0.01, and 0.005 seconds were compared with that of 0.8 seconds. A minimum of 0.2 seconds is currently the fastest commercially available sensing system that suits these purposes. For ease of comparison, the window size was held constant at 50. Both controllers show improved performance with respect to the standard deviation as the sampling period decreases. The adaptive controller, however, shows a greater improvement, 0.0061 μm as compared to the 0.0074 μm of the integral controller at a sampling rate of 0.2 seconds. Table 4 shows a complete breakdown of the results.

Table 4: Controller response simulations at different sampling periods

	Integral		Adaptive	
Sampling Time (s)	Mean Diameter (μm)	Standard Deviation (μm)	Mean Diameter (μm)	Standard Deviation (μm)
0.8	759.7	0.0082	760.1	0.007
0.6	759.7	0.0076	759.9	0.0068
0.4	759.8	0.0074	759.9	0.0062
0.2	759.9	0.0074	759.9	0.0061
0.01	759.9	0.0074	759.9	0.0061
0.005	759.9	0.0074	759.9	0.0061

An inspection of the results between controller simulations provides considerable support for the implementation of the adaptive procedure. In the present configuration the adaptive controller demonstrates superior performance in the simulation even at the lowest window size. The mean droplet diameter was closer to the target diameter in the white noise simulation and the standard deviations of both simulations favored the adaptive controller. The results of window comparisons against the baseline of the integral controller can be seen in Figure 6. Window size has no effect on the integral controller. Above a size of 50, however, the adaptive controller shows a mean diameter jump of 0.2 micrometers to 760 μm. A maximum window size of 100 was used for the purposes of these experiments, but there are undoubtedly physical limitations to window sizing. From the observed results, the response of the adaptive controller improves with increasing window size. This is due to the fact that larger window sizes allow for a larger sample set from which to adapt the breakup frequency. The correlation will need to be established in actual UDS runs to determine a maximum applicable value.

The simulation comparison involving decreasing sampling times also provided additional support for the adaptive control scheme. Figures 7 and 8 show the effects on the mean and standard deviation of droplet diameters for both controllers of decreasing sampling periods. The mean droplet diameter results are not entirely conclusive. Although the adaptive controller levels out faster, an advantageous trait, it appears to undershoot the target diameter by 0.1 microns on average, and that trend appears to continue as the sampling time decreases further. The integral controller shows a steady, albeit slower, improvement towards the target diameter. Both controller simulations level off after a sampling time of 0.2 seconds with respect to the mean diameter. The standard deviation results are more conclusive. The standard deviations of the adaptive controller are smaller than the integral controller at every sampling period. Also, the rate at which the standard deviation decreases is faster for the adaptive controller. The standard deviation improvement seen in the adaptive controller is the result of the continuous store of frequency data on which to adjust the breakup frequency. The integral controller only has one past data point with which to correct the frequency. This implies that, with respect droplet diameter standard deviation, the adaptive system totally outperforms the integral system.

By virtue of the reduced variability in the adaptive controller, there is ample reason to consider further research for implementation. As mentioned above, the advantage of the adaptive controller with respect to decreasing sampling times makes it a superior candidate for expansion potential, especially with the advent of a more structured data acquisition device.

The next step in development should be the codification of the adaptive system into the controlling computer using Visual C++. Should the Gaussian noise be as substantial as believed with respect to white noise, a significant decrease in droplet diameter variation should be observed. A determining factor of the success of the implementation of this algorithm will be the speed at which it is able to carry out its computations. The present codification in MATLAB allows for a frequency update that does not require a major matrix operation, simply a multiplicative one. If that same method is not easily importable into C++, then the insertion of a matrix operation that increases with each iteration could lead to significant processing slowdowns, especially with the advent of a faster data acquisition package.

5. Conclusions and Recommendations

The adaptive controller performs better than the integral controller under all simulated conditions. In the noise simulations, both white and Gaussian, the improvements to the mean droplet diameter are relatively small, on the order of 0.2 μm for the noise simulation comparisons. This alone may not be a significant enough gain to warrant an adoption of the adaptive algorithm into the actual control system of the UDS process. However, the 0.0016 μm decrease in the standard deviation of the adaptive system as compared to the integral system is notable. The smaller standard deviation and slightly closer mean make the adaptive controller a worthwhile change to the UDS control system.

The simulations that involved decreasing the sampling period also lent support for the adaptive control algorithm. As Figures 6 and 7 indicate, performance improvements in both mean and standard deviation are observed in simulations using both control systems. Again, the mean droplet diameter showed a slightly smaller improvement at higher sampling periods under the adaptive regime than it did using the integral system. The standard deviation also decreased as the sampling time decreased. This rate of decrease was similar for both control system simulations, but at every sampling period simulated the adaptive controller standard deviation was at least 0.001 μm smalier. The results of the simulations involving sampling times also show no change between sampling times of 0.2, 0.01, and 0.005 seconds. It is unknown whether this performance lower bound exists or if this is the result of the coding of the simulation.

The issue of window sizing is also of great importance to the strength of the adaptive controller. Not only does a greater window size improve the performance of the controller with respect to both mean and standard deviation of droplet diameters, it also provides another element that could potentially be improved with further research.

In conclusion, the implementation of the adaptive control system into the Uniform Droplet Spray apparatus appears to have numerous definite benefits with few potential pitfalls. The current model for the integral controller provides a very accurate simulation if used within the parameters for which it was designed. Using this baseline, the adaptive controller performs better both in terms of approaching the target diameter and in reducing the variance of droplet diameters. Also, should the sampling period be decreased, the adaptive controller would further outperform the integral system.

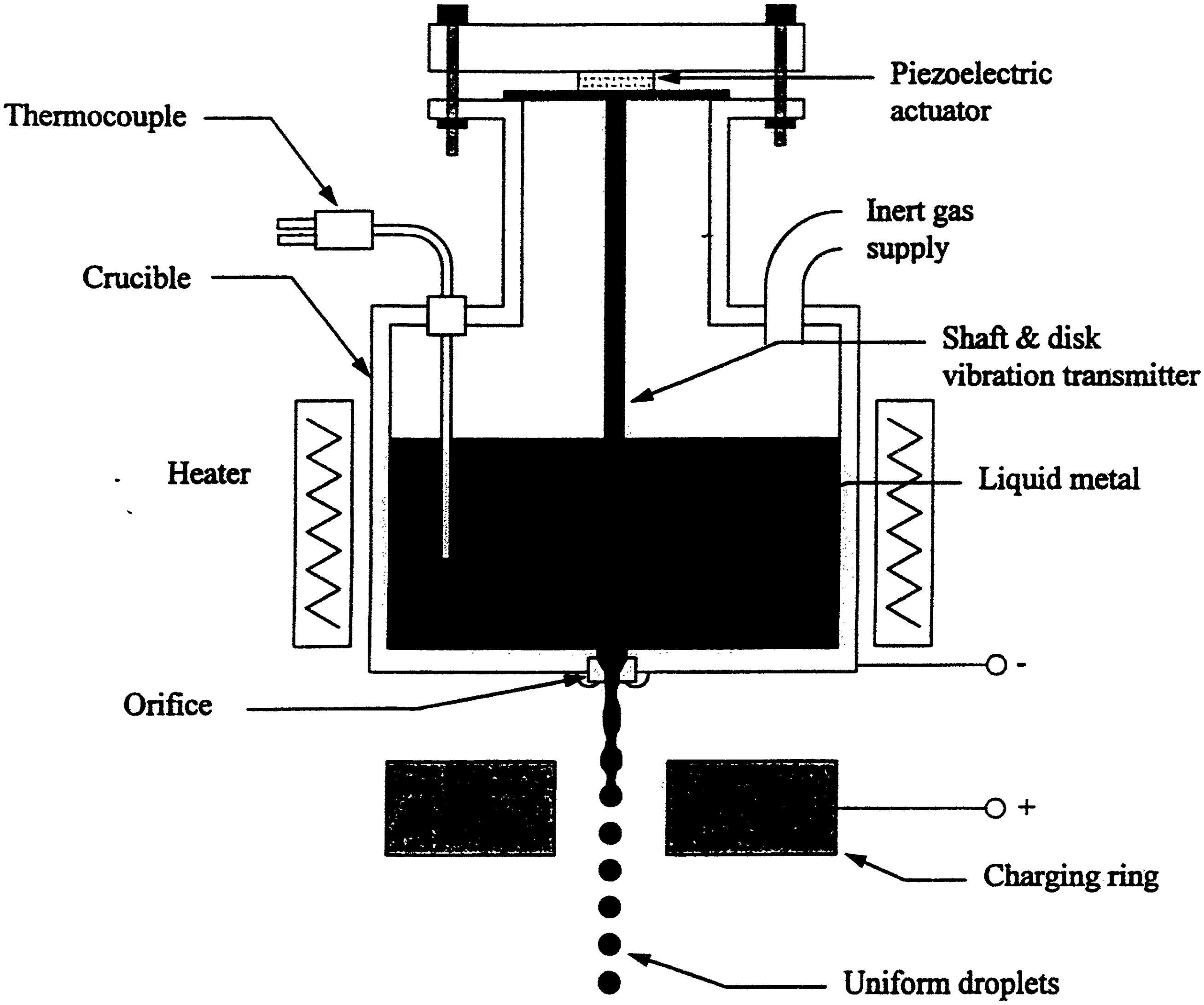

Figure 1: Schematic diagram of a uniform droplet generator

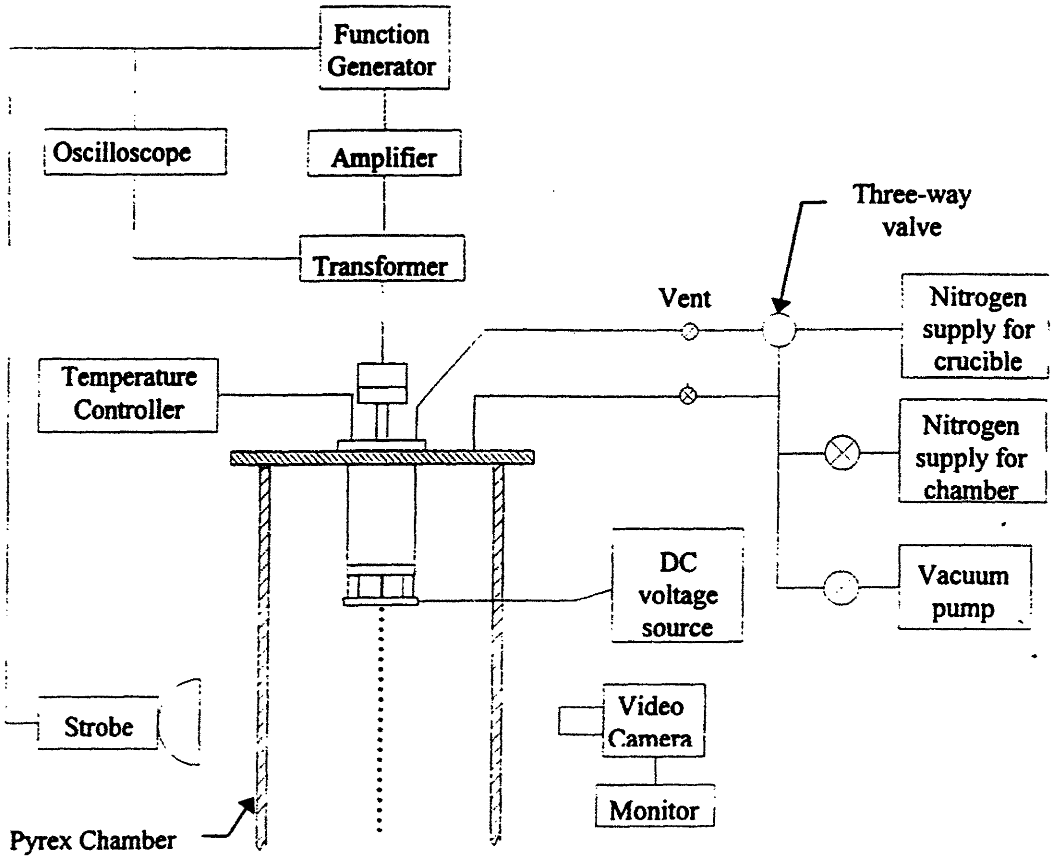

Figure 2: Schematic Diagram of a uniform droplet spray apparatus

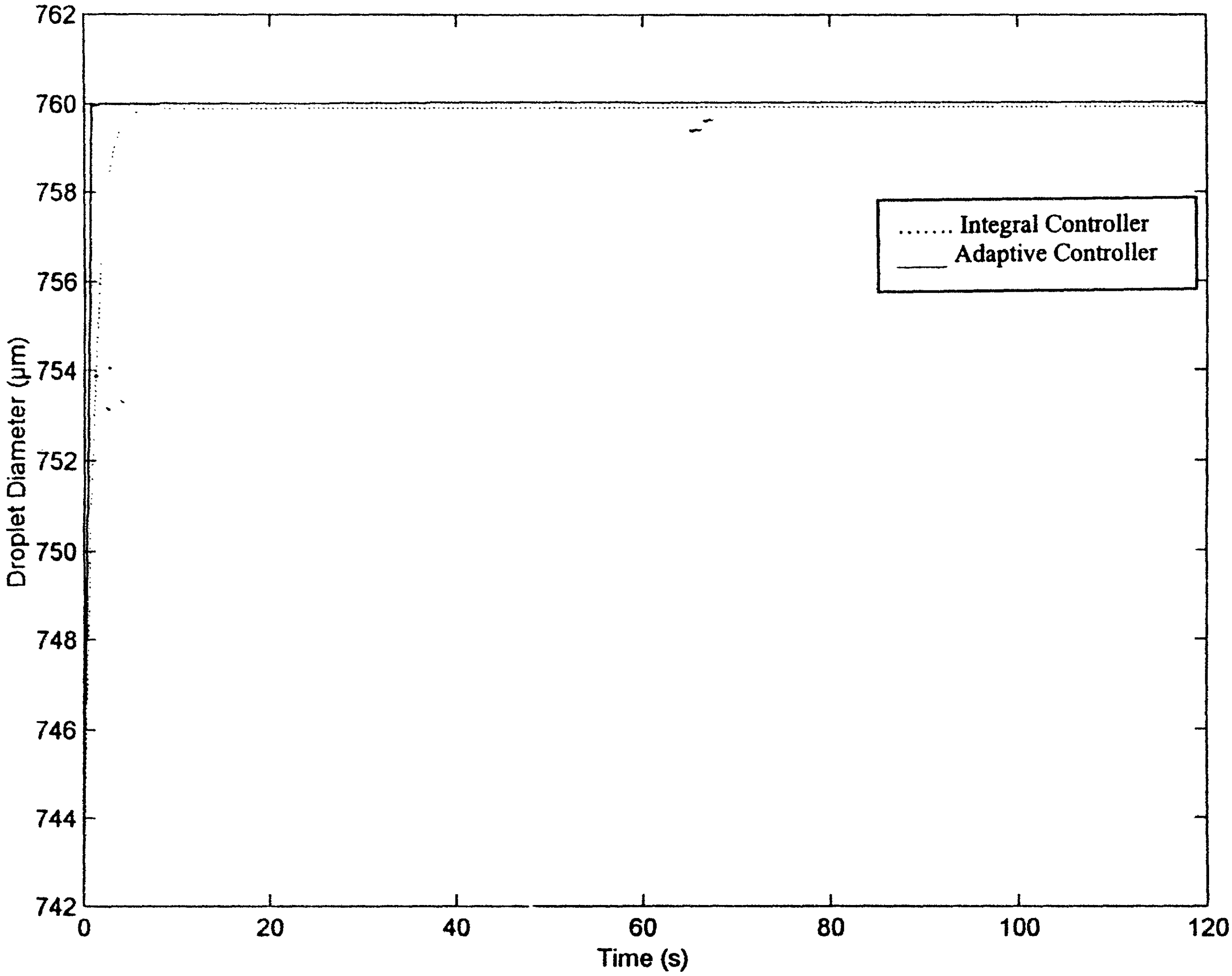

Figure 3: Comparison of an integral controller and an adaptive controller in the absence of noise

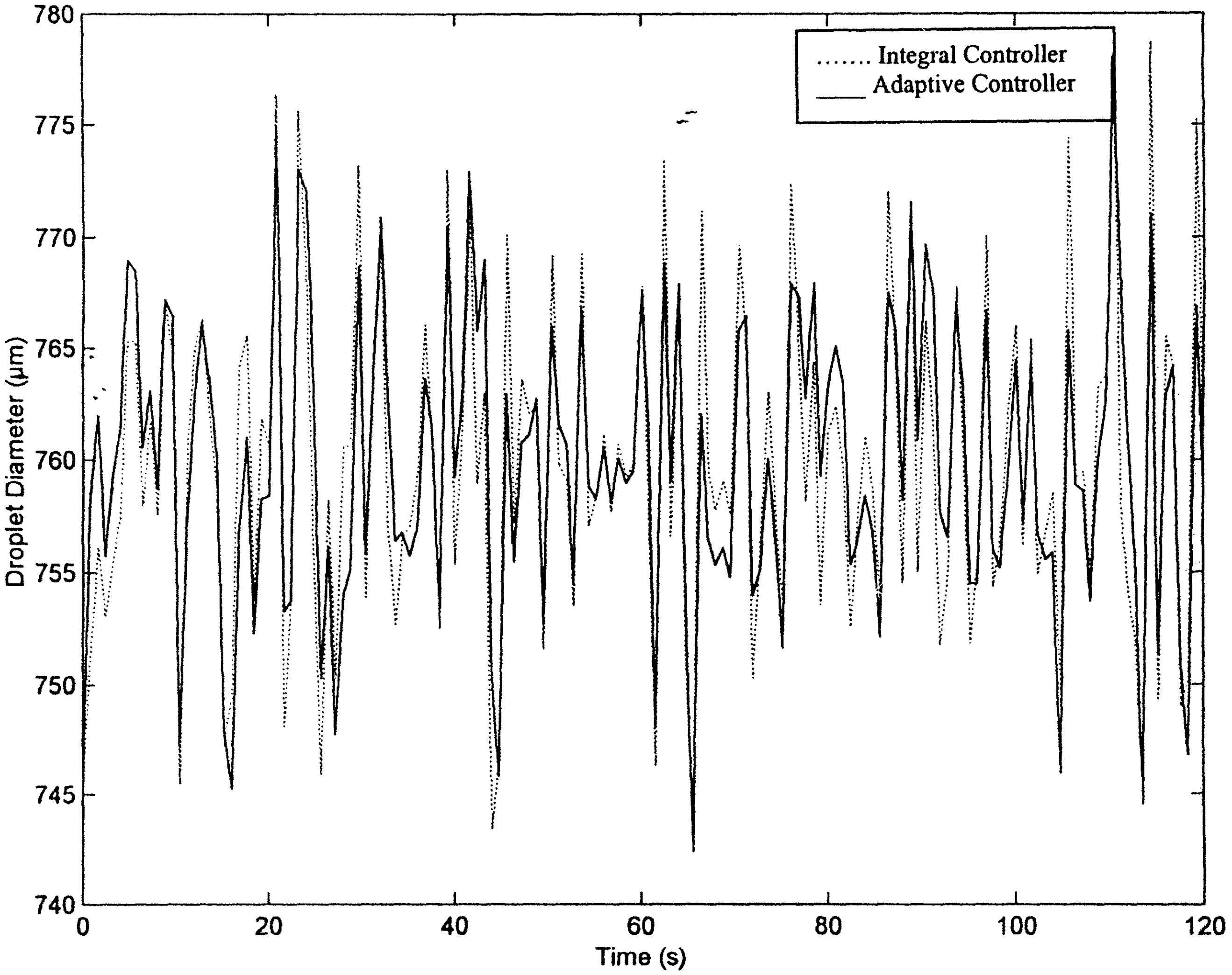

Figure 4: Comparison of an integral controller and an adaptive controller in the presence of white noise

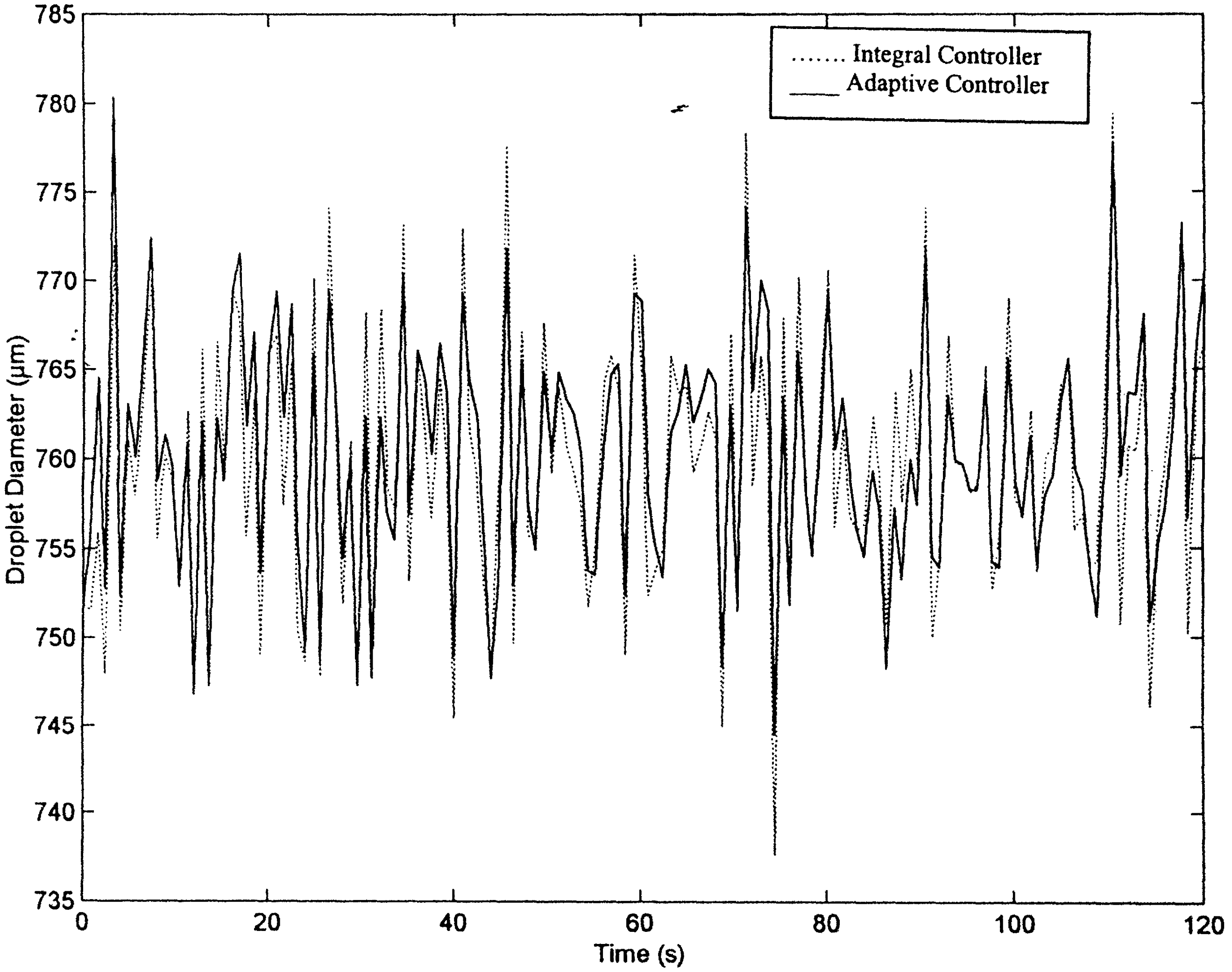

Figure 5: Comparison of an integral controller and an adaptive controller in the presence of Gaussian noise

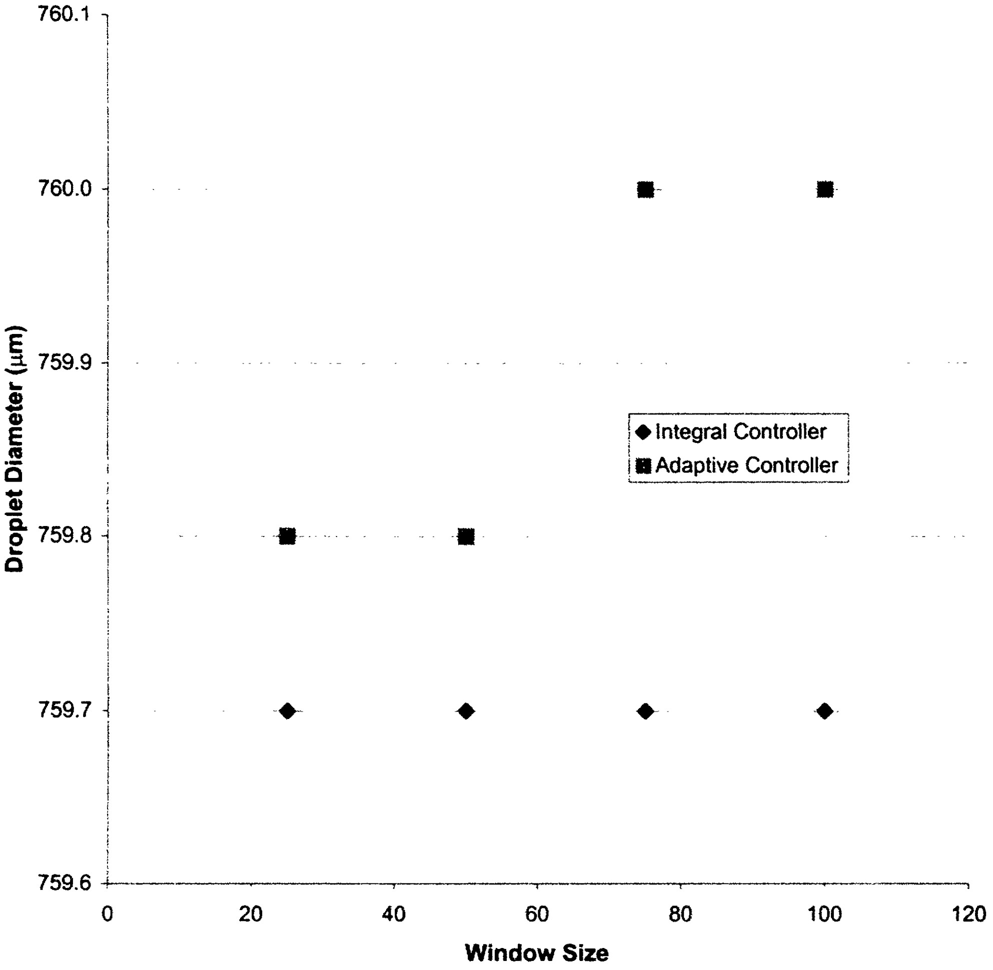

Figure 6: Effects of window sizing on the performance of integral and adaptive controllers. Target size is 760 µm.

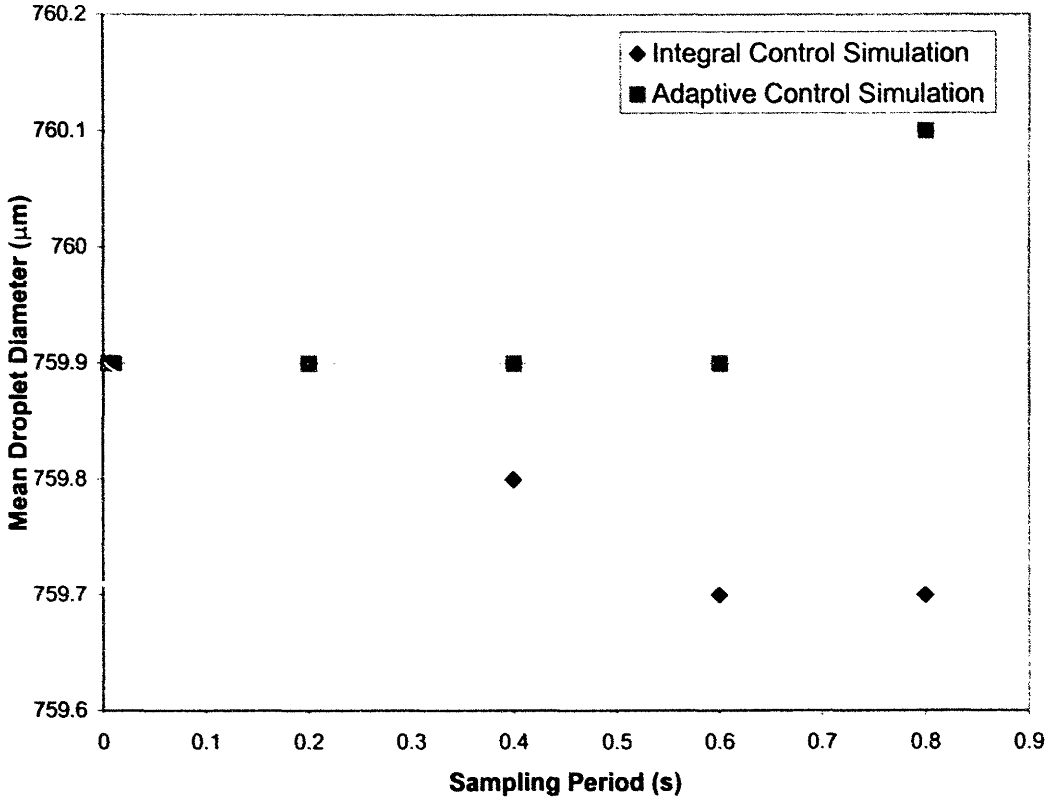

Figure 7: Effects of the sampling time on mean droplet diameters

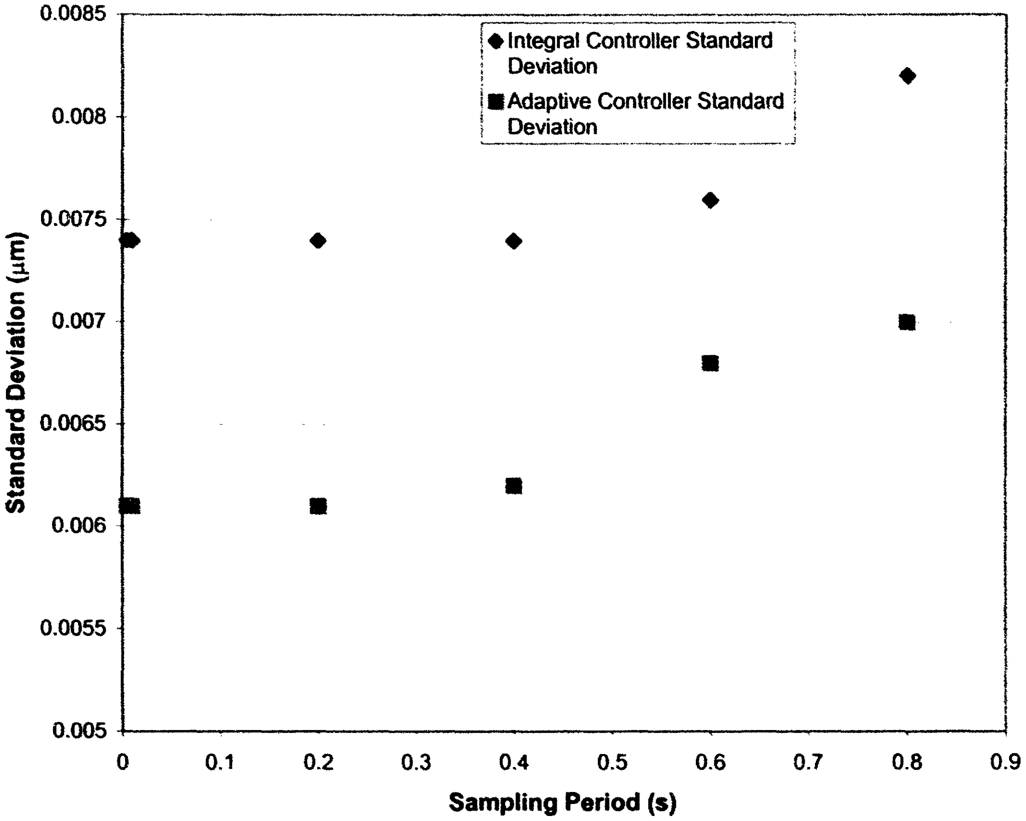

Figure 8: Effects of the sampling time on droplet diameter standard deviations

Bibliography

Chun, J-H, Rocha, J. C., Oh, J-H, "Synthesis and Analysis of a Digital Droplet-Sized Control System." Department of Mechanical Engineering, Massachusetts Institute of Technology, Cambridge, MA, May, 2000.

Kuo, B. C., Automatic Control Systems. Prentice-Hall, Inc., New Jersey, p 54, 1975.

Rocha, J. C., "Control of the UDS Process for the Production of Solder Balls for BGA Electronics Packaging." M.S. Thesis, Department of Mechanical Engineering, Massachusetts Institute of Technology, Cambridge, MA, June, 1997.

Yim, P., "The Role of Surface Oxidation in the Break-Up of Molten metal Jets." Ph.D. Thesis, Department of Mechanical Engineering, Massachusetts Institute of Technology, Cambridge, MA, February, 1996.

Appendix A

The following MATAB code simulates the integral control system in the presence of noise.

```
function curIcont=adap_2(TD,Od,pressure,frequency,mtlkg,time,noise,Ki)

k=1;
g=Ki;
 vi=(mtlkg/8400);
 a=roots([8.017e-3 5.585e-3 1.297e-3 -vi]);
 z0=a(3,1);
 Aj=(((Od*1e-6)^2)*(pi))/4;
 hyp=z0*9.81*8400;
 pressuretot=(pressure*6894.7572)+hyp;
 vel=0.87*(2*pressuretot/8400)^(1/2);
 i=1;
 Q=Aj*vel;
 T=time(1,2);
 for j=time,
  b=(-1.1315e62+(1.06372e31+4.4767e35*Q*j)^2)^(1/2);
  c=1.06372e31+4.67703e35*Q*j;
  z=-0.154819+((1.70243e9)/(c+b)^(1/3))+(3.5198e-12*((c+b)^(1/3)));
  hyp=(z0-z)*9.81*8400;
  pressuretot=(pressure*6894.7572)+hyp;
  vel=0.87*(2*pressuretot/8400)^(1/2);
  w=vel/frequency;
  Ddr=(1+(noise(i)))*(.9848*(6*Aj*w/pi)^(1/3));
  Q=Aj*vel;
  error=(Ddr*1e6)-(TD);
  freq(i,1)=frequency;
  frequency1=frequency;
  frequency=frequency1+(g)*error;
  Dd(i,1)=Ddr;
  zz(i,1)=z0-z;
  ii(i,1)=i;
  vv(i,1)=vel;
  i=1+i;
end

[mean(Dd),std(Dd)]
```

```
plot(time,(Dd*1e6),'b:');
hold off;
%pause
%plot(time,zz);
%pause
%plot(time,freq,'b');
%pause
%plot(ii,Dd);
%pause
%plot(time,vv);
```

Appendix B

The following MATAB code simulates the adaptive control system in the presence of noise.

```
function UDS=adap_1(TD,Od,pressure,frequency,mtlkg,time,noise,ws);

%System initialization
vi=(mtlkg/8400);
a=roots([8.017e-3 5.585e-3 1.297e-3 -vi]);
z0=a(3,1);
Aj=(((Od*1e-6)^2)*(pi))/4;
hyp=z0*9.81*8400;
pressuretot=(pressure*6894.7572)+hyp;
vel=0.87*(2*pressuretot/8400)^(1/2);
Q=Aj*vel;
T=time(1,2);

%Controller initialization
%ws=10; %window size
wv1=ones(ws,1);
wv2=-T*((1:ws)-1)';
wv3=wv2.^2;
wv=[wv1,wv2,wv2,wv3];
wu=zeros(ws,1);
wd=zeros(ws,1);

i=0;
uu=[];
dd=[];

for j=time,
  %Ddr calculation
  b=(-1.1315e62+(1.06372e31+4.4767e35*Q*j)^2)^(1/2);
  c=1.06372e31+4.67703e35*Q*j;
  z=-0.154819+((1.70243e9)/(c+b)^(1/3))+(3.5198e-12*((c+b)^(1/3)));
  hyp=(z0-z)*9.81*8400;
  pressuretot=(pressure*6894.7572)+hyp;
  vel=0.87*(2*pressuretot/8400)^(1/2);
  w=vel/frequency;
  Q=Aj*vel;
  Ddr=(1+noise(i+1))*(.9848*(6*Aj*w/pi)^(1/3));

  %Frequency update
  uu=[uu;frequency^(-1/3)];
  dd=[dd;Ddr];

  ul=length(uu);
  wu=uu(max([1,ul-ws+1]):ul);
  wd=dd(max([1,ul-ws+1]):ul);

  lw=length(wu);
  A=reshape(wv(1:lw,:)'*wu.^6,2,2);
  B=wv(1:lw,[1,2])'*(wu.*wd).^3;
  if i==0
        X=[uu(1)^-6*(uu(1)*Ddr)^3;0];
  else
        X=inv(A)*B;
  end
  frequency=(X(1)-X(2)*lw*T)*(TD*1e-6)^(-3);
  i=1+i;
end

[mean(dd),std(dd)]

plot(time,(dd*1e6),'r');
hold;
```